IEEE Access
Multidisciplinary ⋮ Rapid Review ⋮ Open Access Journal

Received 7 January 2023, accepted 2 February 2023, date of publication 9 February 2023, date of current version 14 February 2023.

Digital Object Identifier 10.1109/ACCESS.2023.3243081

RESEARCH ARTICLE

Parameter Estimation of Fractional-Order Chaotic Power System Based on Lens Imaging Learning Strategy State Transition Algorithm

CHUNYU AI[1], SHAN HE[1,2], AND XIAOCHAO FAN[1,3]

[1]School of Electrical Engineering, Xinjiang University, Ürümqi 830047, China
[2]Engineering Research Center of Ministry of Education for Renewable Energy Generation and Grid Connection Control, Xinjiang University, Ürümqi 830047, China
[3]Xinjiang Institute of Engineering, Ürümqi 830047, China

Corresponding author: Shan He (authorA2741453682@163.com)

This work was supported in part by the Xinjiang Uygur Autonomous Region Key Research and Development Program under Grant 2022B01003-3, in part by the Xinjiang Uygur Autonomous Region Key Laboratory Opening Project under Grant 2022D04029, in part by the Xinjiang Uygur Autonomous Region University Scientific Research Project under Grant XJEDU2021I010, and in part by the National Natural Science Foundation of China under Grant 52266018.

ABSTRACT Parameter identification of fractional-order chaotic power systems is a multidimensional optimization problem that plays a decisive role in the synchronization and control of fractional-order chaotic power systems. In this paper, a state transition algorithm based on the lens imaging learning strategy is proposed for parameter identification of fractional-order chaotic power systems. Taking a fractional-order six-dimensional chaotic power system mathematical model as an example, the mathematical model and chaotic state are analyzed. First, the Tent chaotic mapping is used to initialize the population, thus increasing population diversity. The randomness and ergodicity of the Tent chaotic sequence are used to enhance the global searching ability of the algorithm. Second, a maturity index is employed to determine population maturity. The lens imaging learning strategy is used to suppress the premature convergence of the state transition algorithm effectively and help the population jump out of local optima. Finally, the improved state transition algorithm is used to identify the parameters of the fractional-order six-dimensional chaotic power system model. The proposed improved state transition algorithm shows high estimation accuracy and convergence speed, and is superior to the traditional state transition and particle swarm optimization algorithms. The simulation results show that the parameters of the fractional-order chaotic power system are identified accurately even in the presence of white noise, demonstrating the strong robustness and versatility of the proposed algorithm.

INDEX TERMS Fractional-order chaotic power system, parameter estimation, state transition algorithm, lens imaging learning strategy.

I. INTRODUCTION

The accuracy of parameter estimation is a prerequisite for the safe and stable operation of power grids [1], [2], [3]. As various electronic devices are added as loads to the power system, its behavior starts exhibiting chaotic phenomena [4], [5], which are different from conventional oscillations. These phenomena are likely to cause serious fluctuations in the operation of the power grid and may result in large-scale power system instabilities or even widespread power outages. Controlling the power system when it is in a chaotic state is the key to ensuring the stable operation of the power grid. Obtaining accurate and reliable parameters of the chaotic power system is the basis for realizing chaotic control.

Previous studies have mostly focused on parameter estimation of power systems that operate stably, conventional

The associate editor coordinating the review of this manuscript and approving it for publication was Yilun Shang.

chaotic systems, and integer-order chaotic power systems. However, the parameter identification problem of fraction-order chaotic power systems has more practical theoretical value and broader application prospects than that of integer order chaotic power systems. The introduction of fractional calculus [6] in the early 17th century presented a new research direction for furthering the understanding of integer calculus. Fractional-order modeling can more accurately reflect some complex dynamic characteristics in the fields of natural science and engineering. In the field of electrical engineering, research work using fractional calculus has demonstrated some Interesting results, such as the fractional-order model of permanent magnet synchronous motor [7], [8], the fractional-order model of a power system [9], the ferromagnetic of a fractional-order power system's ferromagnetic resonant chaotic model [10], a fractional RLC circuit model [11], a fractional filter [12], a fractional DC-DC converter [13], a fractional Chua's circuit [14], fractional Maxwell equations for electromagnetic field [15], etc. In recent years, the control of fractional-order chaotic power systems has drawn the attention of experts [16], [17], [18]. But unfortunately, in the real world, the parameters of fractal-order chaotic power systems are not exactly known. It is difficult to control fractious-order chaotic power systems with unknown parameters.

However, with the development of swarm intelligence optimization algorithms, many intelligent algorithms have been applied to the parameter identification of typical fractional chaotic systems. In [19], an improved quantum behavioral particle swarm optimization (PSO) algorithm was proposed for the parameter estimation problem of uncertain fractional-order chaotic systems, and the system parameters and fractional-order derivatives were estimated as independent unknown parameters. Parameter estimation of fractional-order chaotic systems with time delay was studied in [20], which is of great significance to such systems' modeling and control. A numerical algorithm for fractional delay differential equations was presented, which transformed the estimation problem into a nonlinear, multivariate, and multimodal optimization problem. To solve this complex optimization problem effectively, a multi-choice differential evolution algorithm was proposed. In [21], a hybrid artificial bee colony algorithm was proposed for the estimation of the parameters of an unknown fractional-order memristive chaotic system, which transformed parameter estimation into a multi-dimensional optimization problem and treated the fractional-order as an independent variable. In [22], proposed and studied the estimation of fractional chaotic systems of not only unknown order and parameters, but also unknown initial values and structure. Aiming at this problem, a compound differential evolution algorithm was proposed. In [23], different meta-heuristic optimization algorithms were used to estimate the parameters of a fractional-order chaotic system. In [24], problems of unequal order were studied, with different structures and parameter uncertainties of the fractional-order chaotic systems. In that case, a feedback controller was designed and an improved quantum PSO algorithm was proposed to optimize the controller. An improved bird swarm algorithm was proposed in [25], and a fractional chaotic system and a fractional Lorentz system were chosen as two examples for parameter estimation. In [26], a fractional-order chaotic system parameter estimator was proposed based on differential evolution, which treated the order as an additional parameter, and estimated the parameters and the order together by minimizing an objective function. In [27], a fractional cuckoo search algorithm was proposed for the estimation of the corresponding chaotic dynamic behavior parameters in fractional chaos, noisy chaos and hyperchaotic financial systems. In [28] took two typical fractional-order hyperchaotic systems and a fractional-order multi-directional multi-scroll chaotic attractor system as research objects, and proposed a parameter identification method with unknown initial values and a new chaotic particle swarm optimization algorithm.

Most of the above literatures are based on swarm intelligence algorithm for the parameter identification of fractional-order low-dimensional chaotic systems, but it is more valuable to study the parameter identification of fractional-order high-dimensional chaotic systems. Therefore, the parameter identification problem of fractional order six - dimensional chaotic power system is studied in this paper. However, the fractional-order six-dimensional chaotic power system has some problems such as complex oscillation, which makes the parameters of the power system easy to change and easy to be disturbed by the outside world. It is difficult to design a parameter identification method with high accuracy and fast identification speed.

In order to solve the problem of parameter identification of fractional-order chaotic power systems, a method of identification of fractional-order chaotic power systems based on lens imaging learning strategy state transition algorithm is proposed in this paper. Firstly, the chaotic operating state of the fractional-order six-dimensional power system model is analyzed. Then, the unknown parameters are identified by state transition algorithm. Tent chaotic mapping was used to initialize population and maturity index was designed to judge population maturity. The lens imaging learning strategy is added to the basic state transition algorithm to avoid falling into local optimality and increase the population diversity. Finally, the improved state transition algorithm is applied to the parameter identification of fractional-order six-dimensional chaotic power systems.

II. MATHEMATICAL MODEL OF PARAMETER IDENTIFICATION PROBLEM

Consider the n-dimensional fractional-order chaotic power system:

$$D^{q_0} Y = F(Y, Y_0, \theta_0). \tag{1}$$

Here $Y = (y_1, y_2, \ldots, y_n)^T \in R^n$ is the n-dimensional state variable of the system, Y_0 is the initial value of the system,

$q_0 = (q_{01}, q_{02}, \ldots, q_{0n})^{\mathrm{T}}$ represents the fractional order of the original system, and $\theta_0 = (\theta_{01}, \theta_{02}, \ldots, \theta_{0D})^{\mathrm{T}}$ is the vector of the true values of the system parameters. The parameter estimation of the fractional-order chaotic power system can be transformed into a function optimization problem. It is assumed that the reference system is as follows:

$$D^q \hat{Y} = F(\hat{Y}, Y_0, \theta), \tag{2}$$

where $Y = (y_1, y_2, \ldots, y_n)^T \in R^n$ is the n-dimensional state variable of the estimated system, Y_0 is the initial value of the system, $q = (q_1, q_2, \ldots, q_n)^T$ represents the fractional order of the reference system, $\theta = (\theta_1, \theta_2, \ldots, \theta_D)^{\mathrm{T}}$ is the parameter value of the reference system. The estimation principle diagram for a fractional-order chaotic power system is shown in Figure 1, and can be regarded as a multi-dimensional continuous optimization problem. The decision variables are q and θ, and the following fitness function is used:

$$\min J = \frac{1}{L}\sum_{i=1}^{L} ||Y_m - \hat{Y}_m||^2, \tag{3}$$

where L indicates the length of the state variable sequence, $Y_m(m = 1, 2, \ldots, L)$ represents the state variable sequence of the system when the fractional-order chaotic power system evolves under the true value of its parameters, while $\hat{Y}_m(m = 1, 2, \ldots, L)$ represents the state variable sequence of the system when the system evolves under the estimated parameter values.

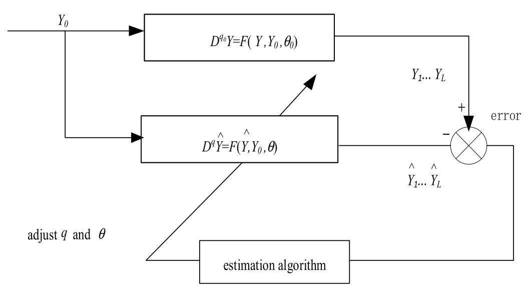

FIGURE 1. Schematic diagram of parameter estimation of fractional-order chaotic power system.

III. LENS IMAGING LEARNING STRATEGIES STATE TRANSITION ALGORITHM

A. STANDARD STATE TRANSITION ALGORITHM

The proposed state transition algorithm(STA) [29] is a typical swarm intelligence optimization algorithm, which has been widely used in many fields [30], [31]. The STA is inspired by modern control theory concepts such as state transition and state space. It treats the solution of the problem to be optimized as a state. Its solution search process is similar to the process of state transition, which is also its main difference from other evolutionary algorithms. The state transition form is defined as

$$\begin{cases} w_{k+1} = A_k w_k + B_k u_k \\ y_k = f(w_{k+1}) \end{cases}, \tag{4}$$

where $w_k \in R^n$ represents a state corresponding to a solution of the problem to be optimized; $A_k, B_k \in R^{n\times n}$ are the state transition matrices, which can be understood as the state transition operators of the optimization algorithm; $u_k \in R^n$ is a function of current and historical states; and f is a fitness function.

To make the state transition operation of the STA controllable when solving the problem, four state transition operators are designed.

1) ROTATION TRANSFORMATION (RT)

$$w_{k+1} = w_k + \alpha\frac{1}{n||w_k||_2}R_r w_k, \tag{5}$$

where α is called the rotation factor; $R_r \in R^{n\times n}$ is a random matrix whose elements follow a uniform distribution in the range; $||w_k||_2$ is the second norm of a vector; The rotation operator causes the generated candidate solution to fall in a hypersphere of radius α.

2) TRANSLATION TRANSFORMATION (TT)

$$w_{k+1} = w_k + \beta R_t \frac{w_k - w_{k-1}}{||w_k - w_{k-1}||_2}, \tag{6}$$

where β is called the translation factor and $R_t \in R$ is a random variable uniformly distributed in the range [0, 1]. The translation search is a line search. It starts from w_k, along the direction pointing to w_k, and the maximum length of the search is β. The translation transformation simplifies one-dimensional searches and balances the global search and the local search.

3) EXPANSION TRANSFORMATION (ET)

$$w_{k+1} = w_k + \gamma R_e w_k, \tag{7}$$

where γ is called the expansion factor and $R_e \in R^{n\times n}$ is a random matrix whose elements follow a Gaussian distribution. This operator is mainly used for global search in the entire space.

4) AXESION TRANSFORMATION (AT)

$$w_{k+1} = w_k + \delta R_a w_k, \tag{8}$$

where δ is called the axesion factor and $R_a \in R^{n\times n}$ is a random diagonal sparse matrix with a single non-zero element at a random position. That element's value is a random variable that follows a Gaussian distribution. The axesion transformation helps improve the single-dimensional search ability.

B. TENT CHAOTIC SEQUENCE

Chaos is a nonlinear phenomenon that is abundantly present in nature. It is characterized by the randomness, ergodicity and regularity of chaotic variables. Many scholars have applied chaotic approaches for search problem optimization, as they allow the maintaining of the diversity of the population and help the algorithms jump out of local optima, resulting in improved global search abilities. The commonly-used Logistic mapping is a typical chaotic system. It can be seen from Figure 2 that its value probability is high in the two ranges [0, 0.1] and [0.9, 1]. The optimization speed of the algorithm is affected by the Logistic ergodic inhomogeneity, and thus the optimization efficiency will decrease. In [32], it was shown that the Tent mapping had better ergodic uniformity and convergence speed than the logistic mapping. It has been proved that the hat Tent map can be used to generate an optimal algorithm's chaotic sequence through strict mathematical reasoning. The Tent mapping expression is:

$$w_{i+1}^D = \begin{cases} 2w_i^D, & 0 \le w_i^D \le \frac{1}{2}, \\ 2(1-w_i^D), & \frac{1}{2} < w_i^D \le 1. \end{cases} \tag{9}$$

By analyzing Tent's chaotic iterative sequence, it can be found that there are short periods and unstable periodic points. To prevent the Tent chaotic sequence from falling into a small periodic point and unstable periodic point during iteration, a random variable rand $(0, 1) \times \frac{1}{N_s}$ is introduced into the original Tent chaotic mapping expression.

The improved Tent chaos mapping expression then becomes as follows:

$$w_{i+1}^D = \begin{cases} 2w_i^D + \text{rand}\,(0,1) \times \frac{1}{N_s}, & 0 \le w_i^D \le \frac{1}{2}, \\ 2(1-w_i^D) + \text{rand}\,(0,1) \times \frac{1}{N_s}, & \frac{1}{2} < w_i^D \le 1. \end{cases} \tag{10}$$

Here, N_s is the number of particles in the sequence, and rand(0, 1) is a random number within the range of [0, 1]. The introduction of the random variables rand$(0, 1) \times \frac{1}{N_s}$ maintains the randomness, ergodicity and regularity of the Tent chaotic mapping. It can also effectively avoid the iteration falling into small and unstable periodic points. The random variable introduced by the algorithm in this paper not only maintains the randomness, but also controls the random value within a certain range to ensure the regularity of the Tent chaotic sequence. Based on the characteristics of the Tent chaos map, in this study, the improved Tent chaos map expression is used to generate a Tent chaos sequence in the feasible domain.

C. MATURITY INDEX DESIGN

Maturity represents the degree of similarity between population individuals. A higher the degree of similarity between individuals corresponds to a higher population maturity. The maturity index is used to judge whether early maturity convergence has occurred and a local optimum has been encountered. If a population has not met the convergence criterion but its maturity is high, this indicates that it may be a case of early maturity due to a local optimum. Since the individuals' degree similarity is defined in a fuzzy manner, a maturity index based on fuzzy theory can fully and accurately reflect the situation of population maturity. In this paper, the fuzzy index is adopted as a maturity evaluation index. The average closeness of the population is used as the maturity index, where a greater average closeness degree of the population corresponds to a greater similarity between individuals and therefore higher maturity. When the average closeness of the population is greater than a threshold, this indicates that the population is aggregating. The individual density in this area is then high, indicating that the average closeness of the population is high. In this case, the population may encountered early maturity due to a local optimum. Let a population of size N_s be located in a search space D. The ith individual's position is $X_i(t) = (x_i^1(t), x_i^2(t), \ldots, x_i^D(t))$ in the tth generation. The iterative process of the ith individual's optimal position experienced is $pbest_i(t) = (pbest_i^1(t), pbest_i^2(t), \ldots, pbest_i^D(t))$. The present positions of all individuals and the optimal positions in the iterative process form an $N_s \times 2D$ order matrix $Q(t)$ as in (11), shown at the bottom of the next page.

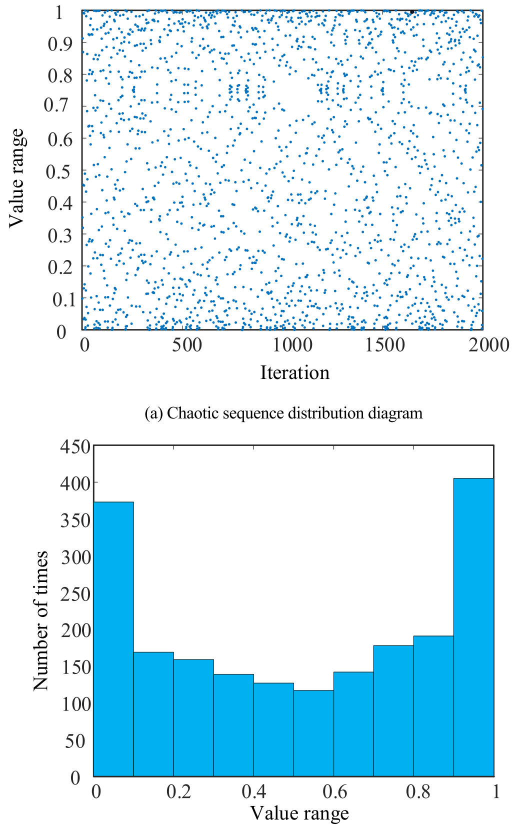

FIGURE 2. Logistic chaotic sequence distribution.

The normalization operation of Eq (11) allows the calculation of the $N_s \times 2D$ order matrix $Q'(t)$:

$$Q'(t)_{uv} = \frac{Q(t)_{uv}(t) - \min\limits_{1 \le n \le N_s, 1 \le d \le 2D} Q_{nd}(t)}{\max\limits_{1 \le n \le N_s, 1 \le d \le 2D} Q(t)_{nd}(t) - \min\limits_{1 \le n \le N_s, 1 \le d \le 2D} Q_{nd}(t)} \tag{12}$$

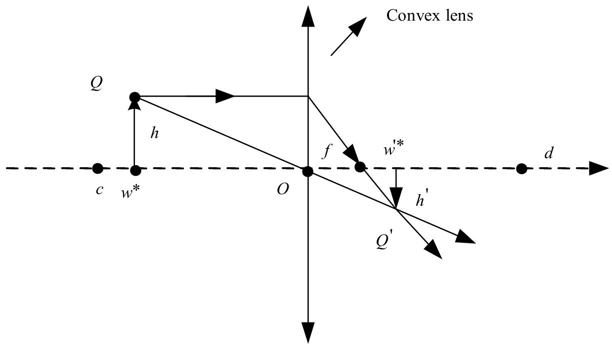

FIGURE 3. Lens imaging learning strategy.

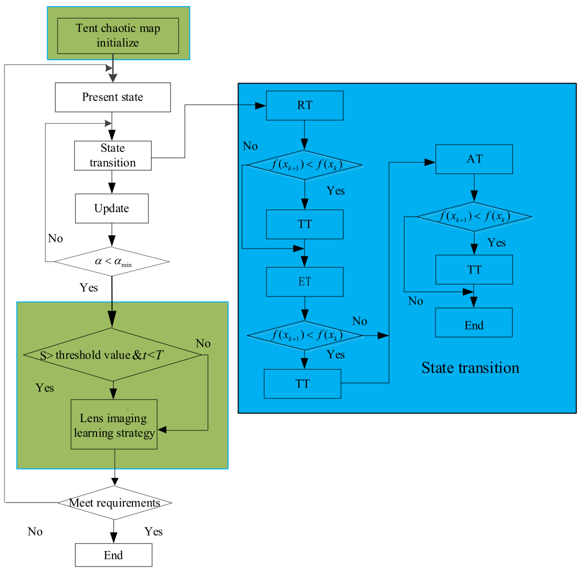

FIGURE 4. Flow chart of improved STA.

Each row vector $Q_i'(t)$ in the matrix $Q'(t)$ represents a fuzzy set. The similarity between any two fuzzy sets $Q_i'(t)$ and $Q_j'(t)$ is represented by the closeness degree in $Q_i'(t)$:

$$\sigma(i,j) = 1 - \frac{1}{2D}\sum_{v=1}^{2D} |q_{iv}'(t) - q_{jv}'(t)|, \tag{13}$$

where $q_{iv}'(t)$ is the vth element of $Q_i'(t)$. Population maturity is represented by the average population closeness degree, which is denoted as:

$$S = \frac{2\sum_{i=1}^{N_s-1}\sum_{j=i+1}^{N_s}\sigma(i,j)}{N_s(N_s-1)} \tag{14}$$

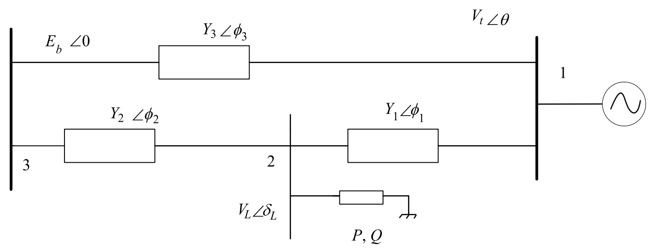

FIGURE 5. Six-dimensional power system model.

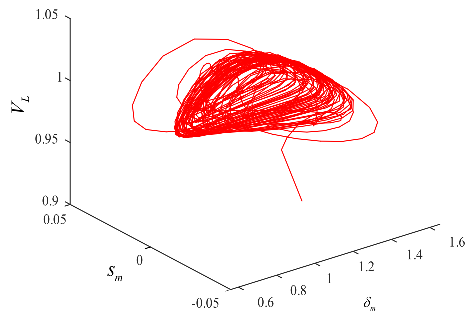

FIGURE 6. Shows Phase trajectory.

The average closeness degree of the population is $0 \leq S \leq 1$, where S stands for population maturity and larger values correspond to more maturity. The average closeness degree of the population can be used to effectively determine whether the population is premature or trapped in a local optimum. If the current iteration number is far smaller than the maximum iteration number, but the average closeness degree of the population is high at this time, this means that the population may be premature or has fallen into a local optimum

D. LENS IMAGING LEARNING STRATEGY

When solving high-dimensional optimization problems, the STA algorithm can easily fall into local optima. To improve the global optimization ability of the basic STA, in this paper the lens imaging learning strategy is applied to STA. The lens imaging learning strategy has been proved to be effective. The introduction of the lens imaging learning strategy expands the effective range of the algorithm group search, thereby reducing the probability of the algorithm falling into local optima. The specific process is as follows:

Basic definition 1. Reverse point: Suppose $W = (w_1, w_2, \ldots, w_D)$ is a point in D-dimensional space, and

$$Q(t) = \begin{bmatrix} x_1^1(t)\; x_1^2(t)\; \cdots x_1^D(t) & pbest_1^1(t) & pbest_1^2(t) & \cdots & pbest_1^D(t) \\ x_2^1(t)\; x_2^2(t)\; \cdots x_2^D(t) & pbest_1^1(t) & pbest_2^2(t) & \cdots pbest_2^D(t) & \\ \vdots\; \vdots\; \ddots\; \vdots & \vdots\vdots & \ddots & \vdots & \\ x_{N_s}^1(t)\; x_{N_s}^2(t)\; \cdots\; x_{N_s}^D(t) & pbest_{N_s}^1(t) & pbest_{N_s}^2(t) & \cdots & pbest_{N_s}^D(t) \end{bmatrix} \tag{11}$$

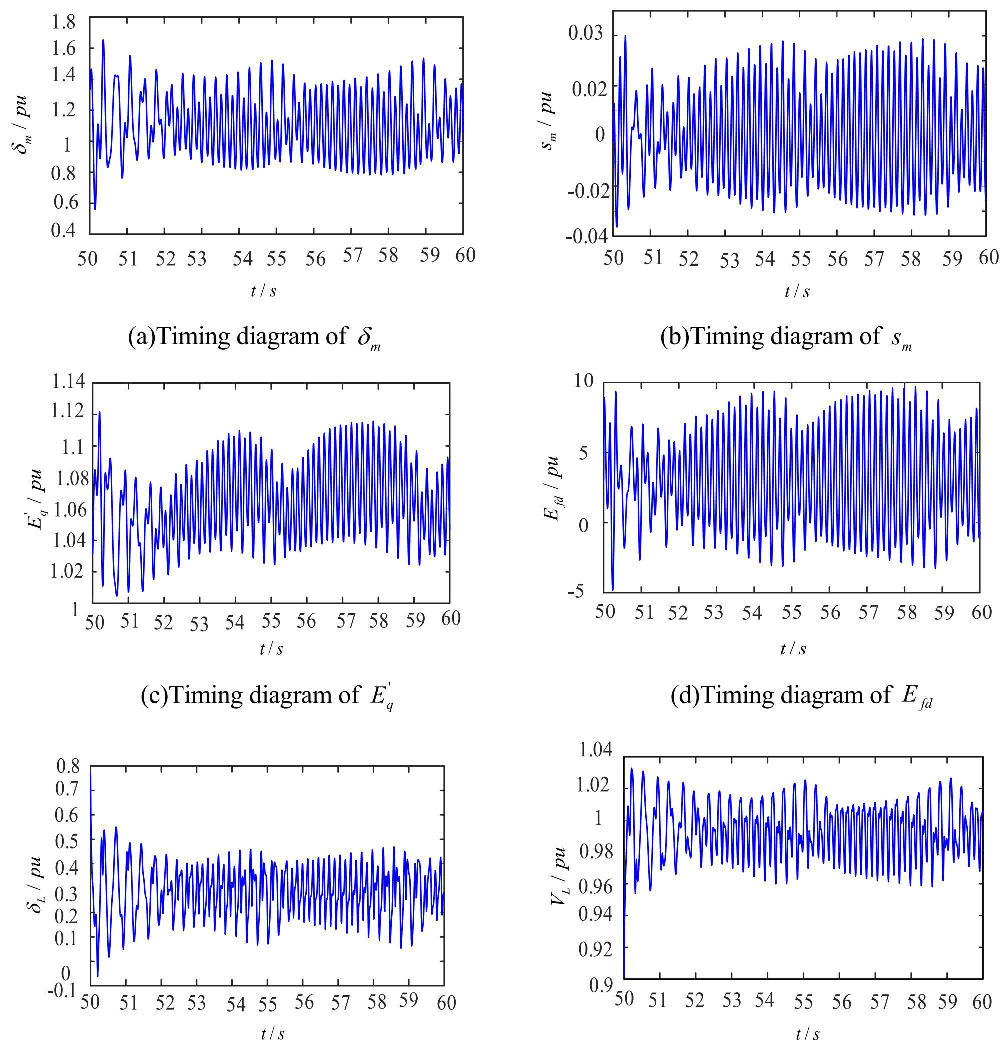

(a)Timing diagram of δ_m (b)Timing diagram of s_m

(c)Timing diagram of E_q' (d)Timing diagram of E_{fd}

(e)Timing diagram of δ_L (f)Timing diagram of V_L

FIGURE 7. State variable timing diagram.

$W_j \in [c_j, d_j], j = 1, 2, \ldots, D$. Then, the reverse point is defined as $W' = (w_1', w_2', \ldots, w_D')$, where $w_j' = c_j + d_j - w_j$.

Basic definition 2. Base point: If there are some points $o_1, o_2, \ldots, o_m$ in the N-dimensional space, the Euclidean distances between any point $W = (w_1, w_2, \ldots, w_D)$ and its reverse point $W' = (w_1', w_2', \ldots, w_D')$ to $o_i(i = 1, 2, \ldots, m)$ are d_i and d_i' respectively. Let $r = \frac{d_i}{d_i'}$, and $r = 1, 2, \ldots, n$; then, o_i is called the base point of W and W' at $r = i$.

Taking a one-dimensional space as an example, suppose there is an individual Q with height h, and its projection on the coordinate axis is the individual w'^*. If a lens of focal length f is placed at the midpoint o of $[c, d]$, an image Q' with a height of h' is obtained through the lens imaging process, and its projection on the coordinate axis is w'^*. The lens imaging learning strategy produces the reverse individual w'^*, as shown in Figure 3.

In Fig. 3, o is used as the base point to obtain the reverse point w'^* of the w^*. This can be derived from the lens imaging principle as follows:

$$\frac{\frac{c+d}{2} - w^*}{w'^* - \frac{c+d}{2}} = \frac{h}{h'} \tag{15}$$

Let $\frac{h}{h'} = r$, where r is called the scaling factor. The calculation equation of the reverse point w'^* can be obtained by transforming Eq. (15):

$$w'^* = \frac{c+d}{2} + \frac{c+d}{2r} - \frac{w^*}{r} \tag{16}$$

When $r = 1$, Eq. (16) can be simplified to:

$$w'^* = c + d - w^*. \tag{17}$$

Eq. (17) is the general reverse learning strategy that acts on w^* and the center position is at $[-\frac{c+d}{2}, \frac{c+d}{2}]$. It can be seen in Eq. (16) and Eq. (17) that the reverse learning strategy is only a special case of the lens imaging learning strategy.

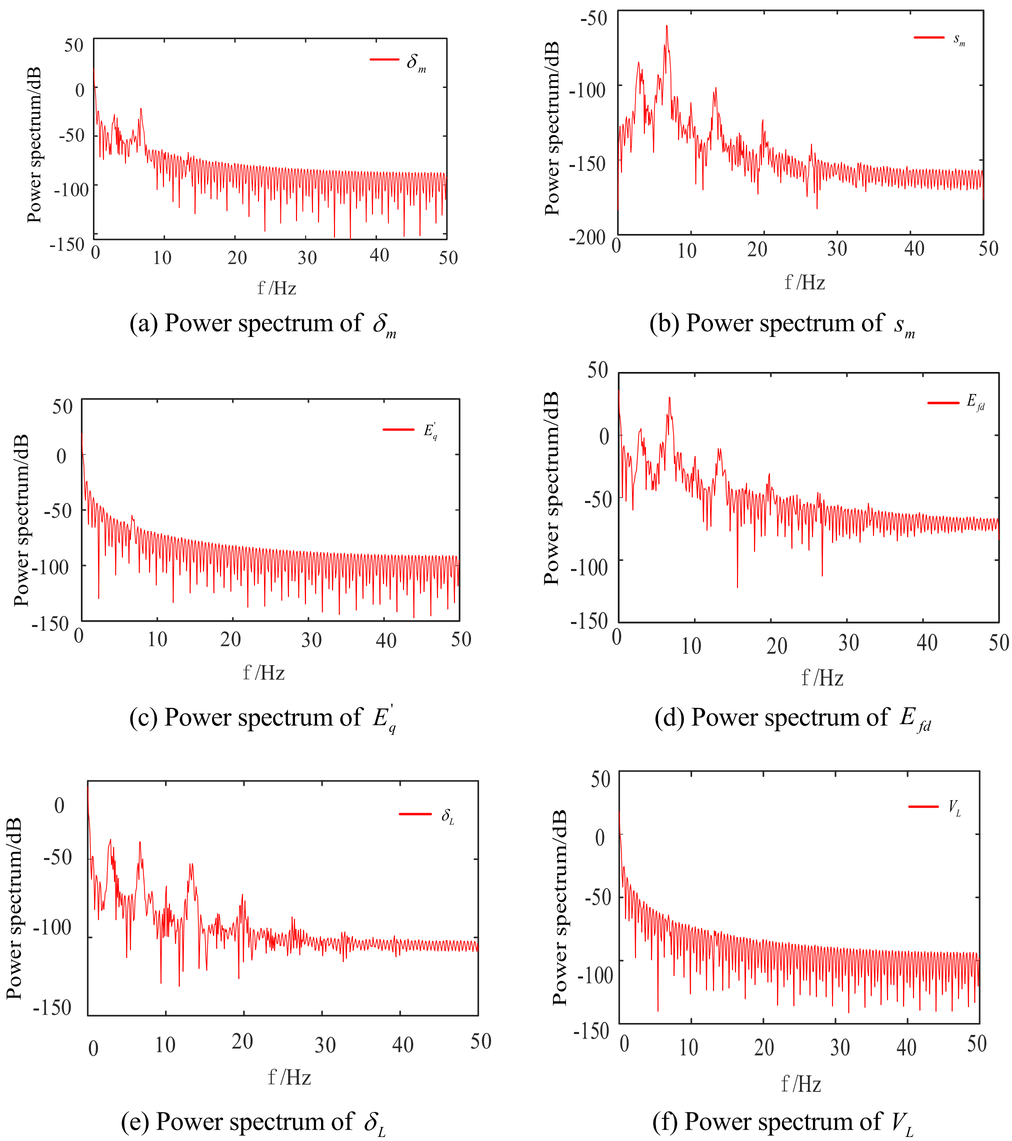

FIGURE 8. **Power spectrum of the fractional-order six-dimensional chaotic power system.**

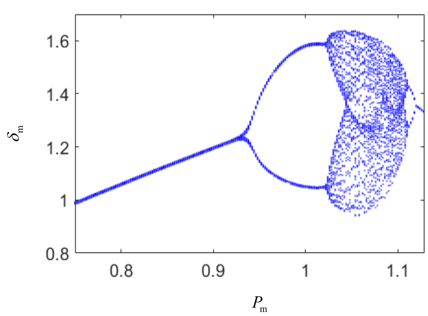

FIGURE 9. **Bifurcation diagram for system state δ_m varying with parameter P_m.**

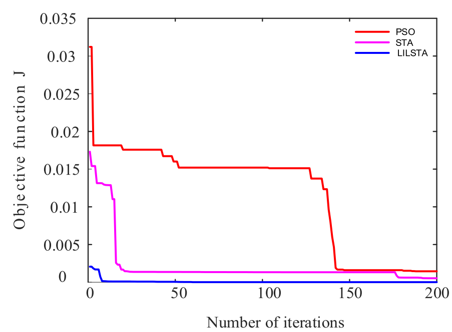

FIGURE 10. **Multi-parameter estimation evolution curve of fractional-order six-dimensional chaotic power system model.**

The new candidate individuals obtained using the lens imaging learning strategy are fixed. By adjusting r, we can change these individuals dynamically, thereby further enhancing the diversity of the group. Generally, the lens imaging learning strategy's principle shown in Eq. (16) can be extended to D-dimensional space

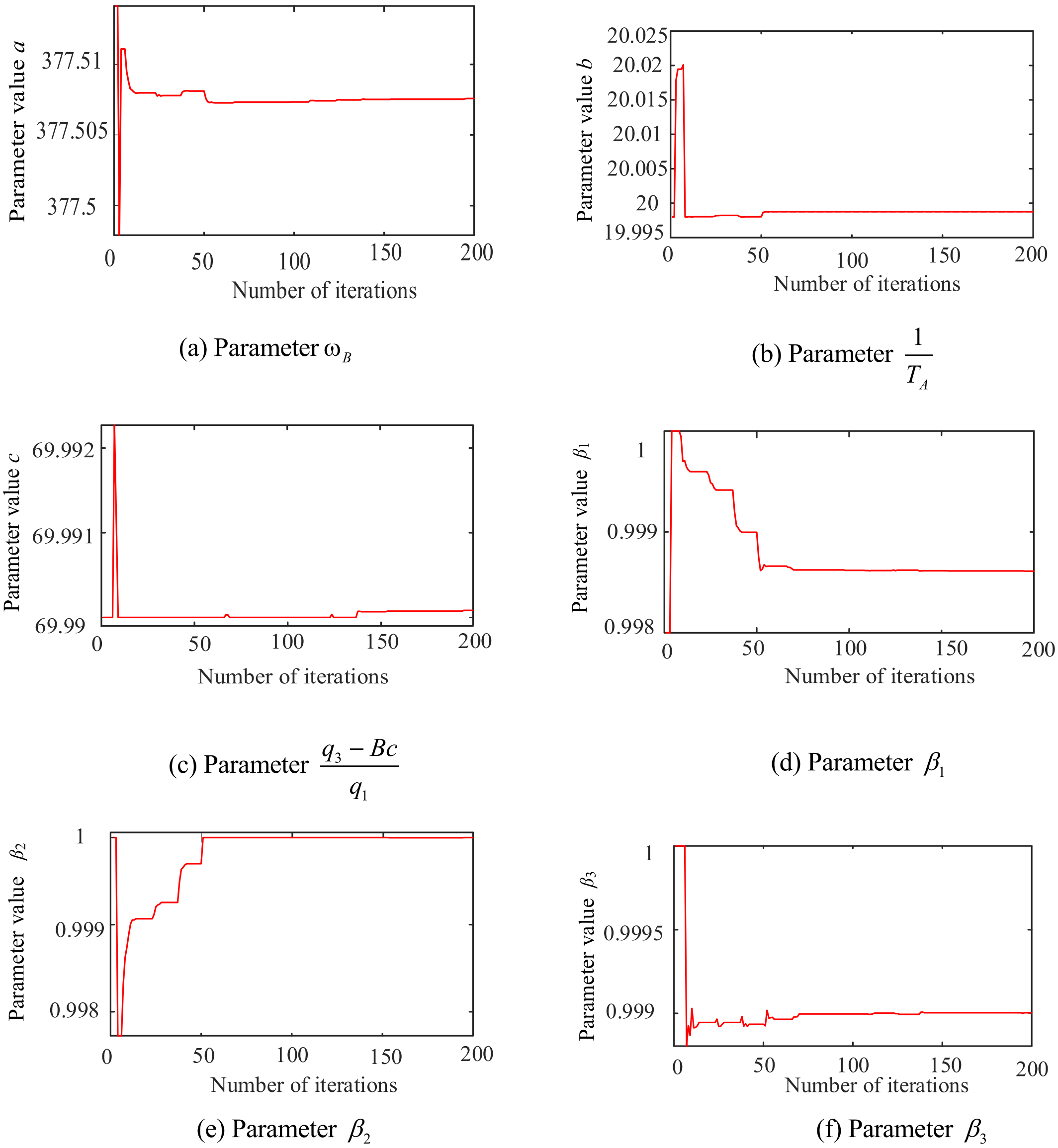

FIGURE 11. Evolution curve of parameter estimation of fractional-order six-dimensional chaotic power system model.

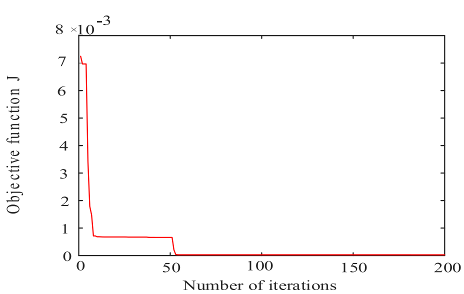

FIGURE 12. Evolution curve of the objective function of the fractional-order six-dimensional chaotic power system model in the presence of noise.

to obtain:

$$w_j'^* = \frac{c_j + d_j}{2} + \frac{c_j + d_j}{2r} - \frac{w_j^*}{r} \tag{18}$$

Here, w_j^* and $w_j'^*$ are the $j-th$ dimensional components of w^* and w'^*, respectively, c_j and d_j are the $j-th$ dimensional components of the upper and lower bounds of the decision variables.

3.5. Parameter identification of chaotic power system based on improved state transition algorithm

In this paper, the Tent chaotic map is used to initialize the population, and the lens imaging learning strategy is used to improve the accuracy and optimization ability of the algorithm. The main steps of the improved STA are as follows:

Step 1: The parameters related to the algorithm are set and the Tent chaotic sequence is improved to generate the initial population. The generated initial population has ergodicity and randomness, which allow it to avoid premature convergence and falling into local optima effectively.

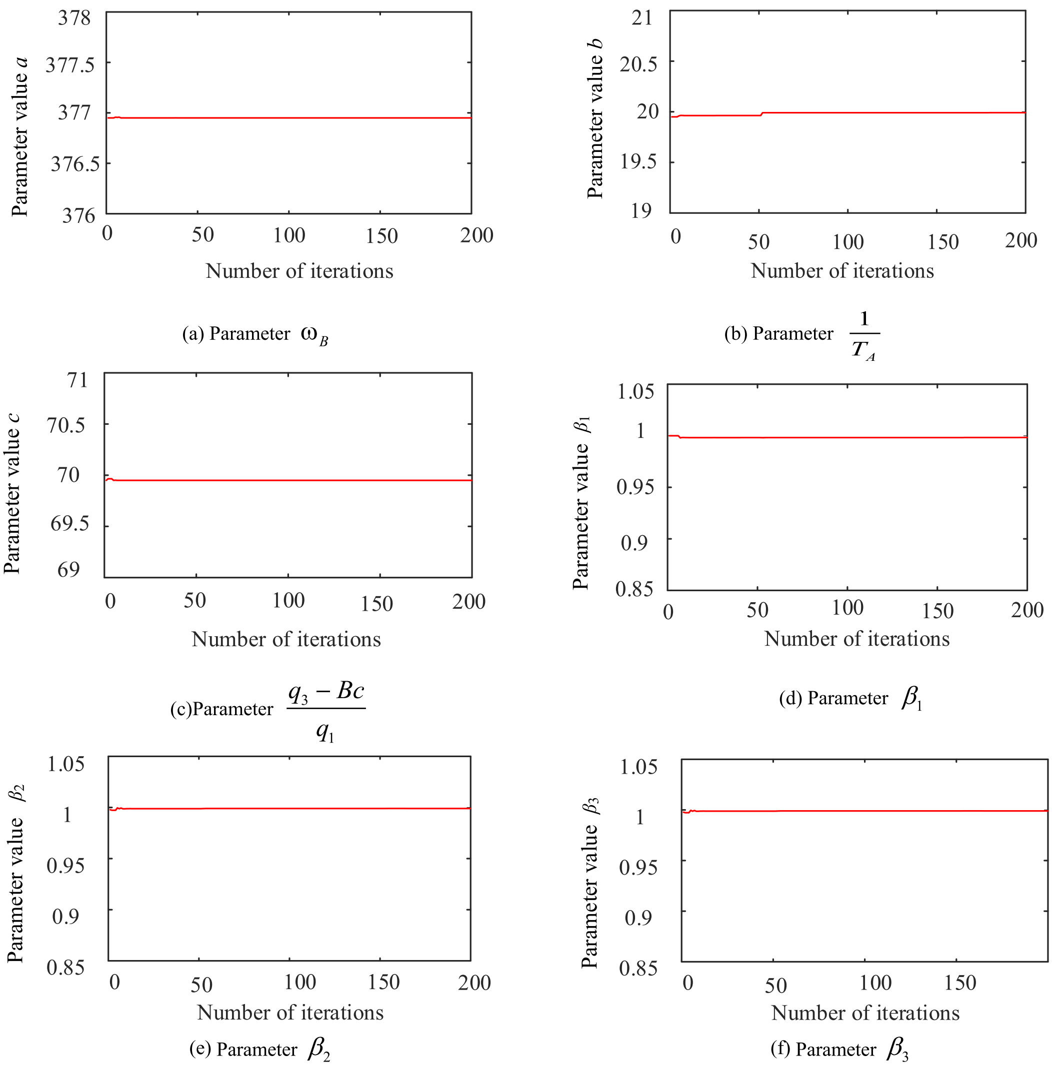

FIGURE 13. Evolution curve of estimated parameter values of fractional-order six-dimensional chaotic power system model in the presence of noise.

Step 2: The fitness function value of each state is counted separately and the solutions and fitness function values corresponding to all current states are recorded;

Step 3: Four transformation operations are performed, the state is updated, the fitness value is recorded and the state is evaluated;

Step 4: The optimal state of the neighborhood is determined, the maturity index is introduced to evaluate the population maturity, and the lens imaging learning strategy is applied. The fitness values of the current and the stored states are compared. If the current fitness value is better, the stored state is updated;

Step 5: Determine whether the requirements are met. If yes, the algorithm ends; otherwise, it returns to step 3.

The flow chart of the improved STA is shown in Figure 4.

IV. POWER SYSTEM MODEL AND CHAOTIC CHARACTERISTICS ANALYSIS BASED ON FRACTIONAL CALCULUS

A. FRACTIONAL CALCULUS

As the field of fractional calculus is continuously explored in scientific and technology applications, the resulting descriptions are becoming more accurate in reflecting the dynamic process of systems encountered in many natural phenomena. The basic operator: ${}_bD_t^\beta$ is described as:

$$
{}_bD_t^\beta = \begin{cases} \frac{d^\beta}{dt^\beta}, & \beta > 0, \\ 1, & \beta = 0, \\ \int_b^t (d\tau)^{-\beta}, & \beta < 0, \end{cases} \tag{19}
$$

where $\beta(\beta \in R)$ is the order, b and t are the bounds of operation. In this paper, Caputo's definition is adopted.

TABLE 1. Identification results of multi-parameter algorithms for fractional-order six-dimensional chaotic power system model.

Algorithm	LILSTA	STA	PSO
Optimal value			
ω_B	376.999000000000	376.000042311529	378.000000000000
$\frac{1}{T_A}$	19.999986763895	19.979260239622	20.023672672130
$\frac{q_3 - Bc}{q_1}$	69.999990000000	69.833918773973	69.900000000000
β_1	0.998999000000	0.999000100000	1.000000000000
β_2	0.998999000000	0.999234261404	0.998290523831
β_3	0.999000710586	0.999192553924	1.000000000000
J	1.3472e-09	3.18e-04	1.51e-03
Average value			
ω_B	376.998000000000	378.000000000000	378.000000000000
$\frac{1}{T_A}$	19.998025560865	20.036728967335	19.999990407305
$\frac{q_3 - Bc}{q_1}$	69.990064130057	70.143053832905	70.009625802788
β_1	0.998819771478	1.000000000000	1.002000000000
β_2	0.999178688121	1.000000000000	1.001000000000
β_3	0.999004792050	0.999219880102	1.000300000000
	1.1702e-06	3.30e-04	1.1e-03
Maximum difference			
ω_B	378.000000000000	377.999988348656	378.000000000000
$\frac{1}{T_A}$	20.017581596944	19.937237188857	20.005036159544
$\frac{q_3 - Bc}{q_1}$	69.990989467400	69.521374689572	70.111232519678
β_1	0.999364889380	0.998955038981	1.003000000000
β_2	0.999758516857	0.996524873179	1.003000000000
β_3	0.999033904118	0.998923378887	0.998431199379
J	7.5291e-05	3.04e-03	1.11e-02

The fractional derivative of $f(t)$ is described as:

$$ {}_bD_t^{\beta} f(t) = \frac{1}{\Gamma(n-\beta)} \int_b^t \frac{f^{(n)}(\tau)}{(t-\tau)^{\beta-n+1}} d\tau, \tag{20} $$

where Γ is the Gamma function, and $n \in N$ is the first integer which is not less than β, $n-1 < \beta < n$,The Laplace transform of the Caputo fractional derivative satisfies:

$$ L\{{}_bD_t^{\beta} f(t)\} = s^{\beta} F(s) - \sum_{k=0}^{n-1} s^{\beta-k-1} f^{(k)}(0), n-1 < \beta < n. \tag{21} $$

For zero initial conditions, the Laplace transform of the fractional derivative has the form:

$$ L\{{}_bD_t^{\beta} f(t)\} = s^{\beta} F(s). \tag{22} $$

The power system studied in this paper is shown in Figure 5. This is a three-bus power system composed of generator bus 1, load bus 2 and slack bus 3. The generator supplies power to the P-Q load. The model was formulated by Rajesh and Padiyar.

The integer order six-dimensional power system was established by Rajesh and Padiyar(1999).The fractional-order

TABLE 2. Parameter estimation results of fractional-order six-dimensional chaotic power system model with noise.

	True value	Optimal estimate	Average estimate	Worst estimate
ω_B	377	377.609205547782	376.999910680063	377.999968101622
$\frac{1}{T_A}$	20	20.012912282605	20.000040855680	19.980743594802
$\frac{q_3-Bc}{q_1}$	70	69.990286867776	69.999044027894	69.705602845088
β_1	1	0.999593594333	0.999039704654	0.998882883748
β_2	1	0.999050633587	0.998957691546	1.000000000000
β_3	1	0.999043544330	0.999001589453	0.999245939519
J		4.19e-05	2.61e-08	8.46e-04

six-dimensional power system model obtained from the integer-order six-dimensional power system in [33] is:

$$\begin{cases} \frac{d^{\beta_1}\delta_m}{dt^{\beta_1}} = \omega_B s_m, \\ \frac{d^{\beta_2}s_m}{dt^{\beta_2}} = -\frac{d}{2H}s_m + \frac{P_m}{2H} - \frac{1}{2H}P_g, \\ \frac{d^{\beta_3}E_q'}{dt^{\beta_3}} = -\frac{1}{T_{d0}'}E_q' + \frac{(x_d-x_d')I_d}{T_{d0}'} + \frac{E_{fd}}{T_{d0}'}, \\ \frac{d^{\beta_4}E_{fd}}{dt^{\beta_4}} = -\frac{E_{fd}}{T_A} + \frac{K_A}{T_A}V_{ref} - \frac{K_A}{T_A}V_t, \\ \frac{d^{\beta_5}\delta_L}{dt^{\beta_5}} = \frac{Q}{q_1} - \frac{Q_{1d}}{q_1} - \frac{Q_0}{q_1} - \frac{q_2}{q_1}V_L - \frac{(q_3-B_c)}{q_1}V_L^2, \\ \frac{d^{\beta_6}V_L}{dt^{\beta_6}} = \frac{P}{p_2} - \frac{P_{1d}}{p_2} - \frac{P_0}{p_2} - \frac{p_1[Q-Q_{1d}-Q_0-q_2V_L-(q_3-B_c)V_L^2]}{p_2q_1} \\ -\frac{p_3}{p_2}V_L. \end{cases} \tag{23}$$

In Eq. (23), P_g, I_d, V, Q, and P are functions of the state variables δ_m, E_q', δ_L and V_L. The meaning of each variable, the assignment of the other parameters of the system, and the initial value of the system state variable can be found in [33]. The expression of each variable is (24)–(28), as shown at the bottom of the next page.

B. ANALYSIS OF CHAOS CHARACTERISTICS

We define $\beta_1, \beta_2, \beta_3, \beta_4, \beta_5, \beta_6$ as the fractional orders. When $P_m = 1.1$, $\beta = \beta_1 = \beta_2 = \beta_3 = \beta_4 = 0.999$, the system enters a chaotic state, and its phase trajectory and time sequence are shown in Figure 6 and Figure 7. As can be seen from Figure 6 and Figure 7, the state variables of chaotic motion are all in irregular periodic chaotic states. A corresponding spectrum diagram can be drawn for each state variable. A spectrum diagram with typical characteristics is also selected here, as shown in Figure 8. As Figure 8 shows, the power spectrum is continuous. The signal contains high DC and low-frequency components, and the power spectrum has broadband noise, which is a typical chaotic behavior characteristic.

Among the parameters of the system, P_m represents the mechanical input power of the generator, which is used as a bifurcation parameter to conduct numerical simulation analysis on the complex dynamic behavior of the system. The parameter interval $P_m \in [0.651.129]$ was selected and the maximum method was used to draw the bifurcation diagram of the system state's δ_m change with parameter P_m, as shown in Figure 9. For fractional six-dimensional power system, with the change of control parameter P_m, the system will experience the system goes through period 1, period 2, period doubling and state of chaos.

V. PARAMETER ESTIMATION OF FRACTIONAL-ORDER CHAOTIC POWER SYSTEM BASED ON THE STA WITH LENS IMAGING LEARNING STRATEGY

A. PARAMETER ESTIMATION OF FRACTIONAL-ORDER CHAOTIC POWER SYSTEM

The experiment was implemented using MATLAB R2019b running on an x64-based processor with a Windows10 operating system. The improved STA was used for the parameter estimation of the fractional-order six-dimensional chaotic power system model to verify the effectiveness of the algorithm. In this paper, the prediction correction method was used to solve fractional differential equations. When $P_m = 1.1$ and $\beta = \beta_1 = \beta_2 = \beta_3 = \beta_4 = 0.999$, the fractional-order six-dimensional power system model enters a chaotic state. We selected multi-parameter estimation, in which ω_B, $\frac{1}{T_A}$, $\frac{q_3-Bc}{q_1}$, β_1, β_2, β_3 in the fractional-order six-dimensional power system model were selected as the parameters to be estimated, with $\omega_B = 370$, $\frac{1}{T_A} = 20$,

$\frac{q_3 - Bc}{q_1} = 70$, $\beta_1 = 0.999$, $\beta_2 = 0.999$, $\beta_3 = 0.999$ being the actual values. The number of iterations was set to 200 and the population size was 60. For the STA algorithm, the rotation factor α was $1 \rightarrow 10^{-4}$, and the values of the rotation, translation, expansion and axesion factors were $1, f_c = 5$. The PSO contraction factor was set to 1.3 and the acceleration factor was set to 1.6. The improved STA (lens imaging learning state transition algorithm, LILSTA), STA, and particle swarm optimization (PSO), were executed independently 15 times to obtain their average, optimal, worst, and fitness function values, as shown in Table 1. The fitness function evolution and parameter estimation curves are shown in Figure 10 and Figure 11, respectively.

It can be seen from Figure 10 that LILSTA quickly achieved convergence and accurate estimation of multiple parameters. Table 1 shows the comprehensive comparison results for the three algorithms. It is evident that in the multi-parameter estimation of the fractional-order six-dimensional chaotic power system, the estimation results of the three algorithms are close to the true values, but those obtained using the LILSTA algorithm are superior to those of the STA, PSO algorithms regardless of the optimal, average, and worst values. The error of LILSTA's parameter estimation of the optimal value reaches 10^{-9}, and even the error of the worst value is as low as 10^{-5}. As shown in Figure 11, the LILSTA algorithm achieves an accurate estimation of multiple parameters. The above results show that LILSTA has a faster search speed and achieves higher accuracy in multi-parameter estimation for the fractional-order six-dimensional chaotic power system model.

B. NOISY PARAMETER ESTIMATION

To appraise the performance of the algorithm on parameter estimation under the influence of noise that is expected to occur in practical applications, we added white noise in the range $[-0.1, 0.1]$ to the system state variables δ_m, s_m, E'_q, E_{fd}, δ_L, V_L and used a predictive corrective method to solve the equation. We used the proposed algorithm to estimate the parameters of the noisy fractional-order six-dimensional chaotic power system. The experiment was run 15 times and the average, best, and worst results were obtained and are shown in Table 2. Figure 12 and Figure 13 show the convergence process of the objective function and estimated parameters, respectively. In the presence of noise, the improved STA can still perform good parameter estimation for the fractional-order six-dimensional chaotic power system model, which reflects its robustness.

VI. CONCLUSION

In this paper, the parameter estimation problem of the fractional-order chaotic power system is transformed into a multi-dimensional function optimization problem. The model and its parameter identification algorithm were studied, and the following conclusions were drawn:

1) the chaotic characteristics of the fractional-order six-dimensional chaotic power system model are analyzed.
2) For the problem of parameter estimation, an initial population obtained via a Tent chaotic mapping was used for the basic STA, as this ensures the ergodicity and uniformity of the initial population. The maturity index is

$$P_g = E'_q I_q + (x'_d - x_q) I_d I_q, \tag{24}$$

$$\begin{cases} I_d = [(\sin\phi - Yx_q)\cdot(YE'_q - a) - b\cdot\cos\phi]/A, \\ I_q = [(\cos\phi(YE'_q - a) + (\sin\phi - Yx'_d)\cdot b]/A, \end{cases} \tag{25}$$

$$\begin{cases} A = [(\cos\phi)^2 + (\sin\phi - Yx_q)(\sin\phi - Yx'_d)], \\ a = E_b Y_3 \cos(\delta_m + \phi - \phi_3) + Y_1 V_L \cos(\delta_L - \delta_m - \phi + \phi_1), \\ b = -E_b Y_3 \sin(\delta_m + \phi - \phi_3) + Y_1 V_L \sin(\delta_L - \delta_m - \phi + \phi_1), \\ Y = \sqrt{(Y_1\cos\phi_1 + Y_3\cos\phi_3)^2 + (Y_1\sin\phi_1 + Y_3\sin\phi_3)^2}, \\ \phi = \arctan[(Y_1\sin\phi_1 + Y_3\sin\phi_3)/(Y_1\sin\phi_1 + Y_3\sin\phi_3)], \end{cases} \tag{26}$$

$$\begin{cases} P = V_t V_L Y_1 \cos(r_1) - V_L^2 Y_1 \cos(\phi_1) + E_b V_L Y_2 \cos(r_2) - V_L^2 Y_2 \cos(\phi_2), \\ Q = V_t V_L Y_1 \sin(r_1) + V_L^2 Y_1 \sin(\phi_1) + E_b V_L Y_2 \sin(r_2) + V_L^2 Y_2 \sin(\phi_2), \\ V_t = \sqrt{V_d^2 + V_q^2}, \end{cases} \tag{27}$$

$$\begin{cases} V_d = -x_q I_q, \\ V_q = E'_q + x'_d I_d, \\ r_1 = \delta_t - \theta - \phi_1, \\ \theta = \delta_m + \arctan(V_d/V_q), \\ r_2 = \delta_L - \phi_2. \end{cases} \tag{28}$$

designed to evaluate the maturity of the population, and the convergence speed and optimization accuracy were significantly improved using the lens imaging learning strategy. This approach results in both excellent search performance and development performance.

3) Finally, the proposed improved STA is used for the parameter estimation of a fractional-order six-dimensional chaotic power system model, and its performance is compared with that of the STA, and PSO algorithms. From the results of the comparison experiments, it is evident that the improved STA can solve the fractional-order six-dimension chaotic power system model parameter estimation problem, and achieves higher estimation accuracy.
4) For the fractional-order six-dimensional chaotic power system model under consideration, the estimated parameters were very close to the real

values under both ideal and noisy conditions, showing the effectiveness, robustness and versatility of this algorithm. However, the impact of real-world noise (such as color noise [34] and Levy noise [35]) on power systems is worth studying and is another promising direction.

REFERENCES

[1] V. Khramenkov, A. Dmitrichev, and V. Nekorkin, "Partial stability criterion for a heterogeneous power grid with hub structures," *Chaos, Solitons Fractals*, vol. 152, Nov. 2021, Art. no. 111373, doi: 10.1016/j.chaos.2021.111373.

[2] Z. Jiang, R. Li, A. Li, and C. Ji, "Runoff forecast uncertainty considered load adjustment model of cascade hydropower stations and its application," *Energy*, vol. 158, pp. 693–708, Sep. 2018, doi: 10.1016/j.energy.2018.06.083.

[3] L. Zhang, X. S. Liu, J. W. Pang, D. G. Xu, and V. C. M. Leung, "Reliability and survivability analysis of artificial cobweb network model used in the low-voltage power-line communication system," *IEEE Trans. Power Del.*, vol. 31, no. 5, pp. 1980–1988, Oct. 2016, doi: 10.1109/tpwrd.2015.2426205.

[4] N. V. Stankevich, A. P. Kuznetsov, and E. P. Seleznev, "Chaos and hyperchaos arising from the destruction of multifrequency tori," *Chaos, Solitons Fractals*, vol. 147, Jun. 2021, Art. no. 110998, doi: 10.1016/j.chaos.2021.110998.

[5] D. Yan, L. Wang, S. Duan, J. Chen, and J. Chen, "Chaotic attractors generated by a memristor-based chaotic system and Julia fractal," *Chaos, Solitons Fractals*, vol. 146, May 2021, Art. no. 110773, doi: 10.1016/j.chaos.2021.110773.

[6] J. T. Machado, V. Kiryakova, and F. Mainardi, "Recent history of fractional calculus," *Commun. Nonlinear Sci. Numer. Simul.*, vol. 16, no. 3, pp. 1140–1153, 2011.

[7] D. Peng, K. H. Sun, and A. O. A. Alamodi, "Dynamics analysis of fractional-order permanent magnet synchronous motor and its DSP implementation," *Int. J. Modern Phys. B*, vol. 33, no. 6, Mar. 2019, Art. no. 1950031, doi: 10.1142/s0217979219500310.

[8] P. Mani, R. Rajan, L. Shanmugam, and Y. H. Joo, "Adaptive fractional fuzzy integral sliding mode control for PMSM model," *IEEE Trans. Fuzzy Syst.*, vol. 27, no. 8, pp. 1674–1686, Aug. 2019.

[9] C. Liu, W.-Z. Wu, W. Xie, and J. Zhang, "Application of a novel fractional grey prediction model with time power term to predict the electricity consumption of India and China," *Chaos, Solitons Fractals*, vol. 141, Dec. 2020, Art. no. 110429, doi: 10.1016/j.chaos.2020.110429.

[10] N. Yang, Y. Han, C. Wu, R. Jia, and C. Liu, "Dynamic analysis and fractional-order adaptive sliding mode control for a novel fractional-order ferroresonance system," *Chin. Phys B*, vol. 26, no. 8, Jul. 2017, Art. no. 080503.

[11] K. Haška, D. Zorica, and S. M. Cvetićanin, "FractionalRLCcircuit in transient and steady state regimes," *Commun. Nonlinear Sci. Numer. Simul.*, vol. 96, May 2021, Art. no. 105670, doi: 10.1016/j.cnsns.2020.105670.

[12] M. C. Tripathy, K. Biswas, and S. Sen, "A design example of a fractional-order Kerwin–Huelsman–Newcomb biquad filter with two fractional capacitors of different order," *Circuits, Syst., Signal Process.*, vol. 32, no. 4, pp. 1523–1536, Jan. 2013.

[13] A. G. Radwan, A. A. Emira, A. M. AbdelAty, and A. T. Azar, "Modeling and analysis of fractional order DC-DC converter," *ISA Trans.*, vol. 82, pp. 184–199, 2017, doi: 10.1016/j.isatra.2017.06.024.

[14] F. Yang and P. Li, "Characteristics analysis of the fractional-order chaotic memristive circuit based on Chua's circuit," *Mobile Netw. Appl.*, vol. 26, no. 5, pp. 1862–1870, Oct. 2021, doi: 10.1007/s11036-019-01294-8.

[15] E. K. Jaradat, R. S. Hijjawi, and J. M. Khalifeh, "Maxwell's equations and electromagnetic Lagrangian density in fractional form," *J. Math. Phys.*, vol. 53, no. 3, Mar. 2012, Art. no. 033505.

[16] K. Rajagopal, A. Karthikeyan, P. Duraisamy, R. Weldegiorgis, and G. Tadesse, "Bifurcation, chaos and its control in a fractional order power system model with uncertainties," *Asian J. Control*, vol. 21, no. 1, pp. 184–193, Jan. 2019, doi: 10.1002/asjc.1826.

[17] F. Min, Y. Wang, and Y. P. Dou, "Analysis and control of chaotic oscillation in fractional-order power system with excitation model," *J. Electron Inf. Techn.*, vol. 39, no. 8, pp. 1993–1999, Aug. 2017, doi: 10.11999/JEIT161398.

[18] M. P. Aghababa, "Finite-time chaos control and synchronization of fractional-order nonautonomous chaotic (hyperchaotic) systems using fractional nonsingular terminal sliding mode technique," *Nonlinear Dyn.*, vol. 69, nos. 1–2, pp. 247–261, 2012, doi: 10.1007/s11071-011-0261-6.

[19] J. Wei, Y. Yu, and D. Cai, "Identification of uncertain incommensurate fractional-order chaotic systems using an improved quantum-behaved particle swarm optimization algorithm," *J. Comput. Nonlinear Dyn.*, vol. 13, no. 5, Mar. 2018, Art. no. 051004, doi: 10.1115/1.4039582.

[20] F. Liu, X. Li, X. Liu, and Y. Tang, "Parameter identification of fractional-order chaotic system with time delay via multi-selection differential evolution," *Syst. Sci. Control Eng.*, vol. 5, no. 1, pp. 42–48, Jan. 2017, doi: 10.1080/21642583.2016.1275876.

[21] W. Gu, Y. Yu, and W. Hu, "Parameter estimation of unknown fractional-order memristor-based chaotic systems by a hybrid artificial bee colony algorithm combined with differential evolution," *Nonlinear Dyn.*, vol. 84, no. 2, pp. 779–795, Apr. 2016.

[22] W. Du, Q. Miao, L. Tong, and Y. Tang, "Identification of fractional-order systems with unknown initial values and structure," *Phys. Lett. A*, vol. 381, no. 23, pp. 1943–1949, Jun. 2017.

[23] D. A. Yousri, A. M. AbdelAty, L. A. Said, A. S. Elwakil, B. Maundy, and A. G. Radwan, "Parameter identification of fractional-order chaotic systems using different Meta-heuristic optimization algorithms," *Nonlinear Dyn.*, vol. 95, no. 3, pp. 2491–2542, Feb. 2019, doi: 10.1007/s11071-018-4703-2.

[24] R.-G. Li and H.-N. Wu, "Adaptive synchronization control based on QPSO algorithm with interval estimation for fractional-order chaotic systems and its application in secret communication," *Nonlinear Dyn.*, vol. 92, no. 3, pp. 935–959, May 2018.

[25] P. Zhang, R. Y. Yang, R. H. Yang, G. Ren, and X. Z. Yang, "Parameter estimation for fractional-order chaotic systems by improved bird swarm optimization algorithm," *Int. J. Modern Phys. C*, vol. 30, 2019, doi: 10.1142/s0129183119500864.

[26] Y. Tang, X. Zhang, C. Hua, L. Li, and Y. Yang, "Parameter identification of commensurate fractional-order chaotic system via differential evolution," *Phys. Lett. A*, vol. 376, no. 4, pp. 457–464, 2012.

[27] D. Yousri and S. Mirjalili, "Fractional-order cuckoo search algorithm for parameter identification of the fractional-order chaotic, chaotic with noise and hyper-chaotic financial systems," *Eng. Appl. Artif. Intell.*, vol. 92, Jun. 2020, Art. no. 103662, doi: 10.1016/j.engappai.2020.103662.

[28] Y. Peng, K. Sun, S. He, and X. Yang, "Parameter estimation of a complex chaotic system with unknown initial values," *Eur. Phys. J. Plus*, vol. 133, no. 8, p. 305, Aug. 2018, doi: 10.1140/epjp/i2018-12091-1.

[29] X. Zhou, C. Yang, and W. Gui, "State transition algorithm," *J. Ind. Manage. Optim.*, vol. 8, no. 4, pp. 1039–1056, 2012.

[30] Z. Huang, C. Yang, X. Zhou, and S. Yang, "Energy consumption forecasting for the nonferrous metallurgy industry using hybrid support vector regression with an adaptive state transition algorithm," *Cognit. Comput.*, vol. 12, no. 2, pp. 357–368, Mar. 2020, doi: 10.1007/s12559-019-09644-0.

[31] Y. Dong et al., "A novel hybrid model based on Bernstein polynomial with mixture of Gaussians for wind power forecasting," *Appl. Energy*, vol. 286, 2021, Art. no. 116545, doi: 10.1016/j.apenergy.2021.116545.

[32] L. Shan et al., ''Chaotic optimization algorithm based on Tent map,'' *Control Decis.*, vol. 20, no. 2, pp. 179–182, 2005.

[33] J. Wang, L. Liu, C. Liu, Z. Zhu, and Y. Wang, ''Chaos control in six-dimensional power system via adaptive synergetic approach,'' *J. Vibrat. Control*, vol. 26, nos. 9–10, pp. 790–800, May 2020, doi: 10.1177/1077546319889850.

[34] Z. Liao, K. Ma, S. Tang, M. S. Sarker, H. Yamahara, and H. Tabata, ''Phase locking of ultra-low power consumption stochastic magnetic bits induced by colored noise,'' *Chaos, Solitons Fractals*, vol. 151, Oct. 2021, Art. no. 111262, doi: 10.1016/j.chaos.2021.111262.

[35] Z. Liao, K. Ma, S. Tang, M. S. Sarker, H. Yamahara, and H. Tabata, ''Influence of Levy noise on subthreshold synchronization of spintronic stochastic neurons,'' *Results Phys.*, vol. 27, Aug. 2021, Art. no. 104475, doi: 10.1016/j.rinp.2021.104475.

CHUNYU AI received the M.E. degree in control science and control engineering from Xinjiang University, China, in 2019, where he is currently pursuing the Ph.D. degree with the Electrical Engineering Department. His research interests include chaos control of wind power systems, chaos control of power systems, parameter identification, and wind power prediction.

SHAN HE received the Ph.D. degree from Xinjiang University, Ürümqi, China, in 2006. He is currently working as a Professor with the School of Electrical Engineering, Xinjiang University. His current research interests include renewable energy generation and parameter identification.

XIAOCHAO FAN received the Graduate degree majoring in electrical engineering from Xinjiang University, in 2016. He is currently pursuing the Ph.D. degree. He is also a Professor. He is also a Master's Supervisor. His research interests include new energy generation technology, energy storage technology, and integrated energy systems.